



Fuzzy Adaptive Control Law for Trajectory Tracking Based on a Fuzzy Adaptive Neural PID Controller of a Multi-rotor Unmanned Aerial Vehicle

Abigail María Elena Ramírez Mendoza  and Wen Yu* 

Abstract: This article presents a fuzzy adaptive control law (FACL) designed for tracking the trajectory of a low-scale unmanned aerial vehicle (UAV), based on a new fuzzy adaptive neural proportional integral derivative (FANPID) controller. FACL estimates the angles of rotation, if the reference trajectory is proposed, applying the adaptivity of the new FANPID-Lyapunov controller. UAV parameters were previously identified using the fuzzy adaptive neurons (FAN) method and experimental aerodynamic data. FANPID-Lyapunov controller optimizes trajectory tracking and stability analysis is performed. The FACL simulation results obtained in Matlab[®]/Simulink show the effectiveness, adaptivity and optimization of the flight control system, because it self-tunes the angles satisfactorily, adapts the gains and parameter for the FANPID-Lyapunov-Fuzzy controller, and reduces the error considerably compared to the controllers PID-Fixed gains, PID-Fuzzy adaptive gains, PID-Lyapunov-Fixed gains, and FOPID-Lyapunov-Fuzzy adaptive gains and parameters.

Keywords: FANPID, fuzzy adaptive control law, fuzzy adaptive neurons, stability analysis, trajectory tracking, unmanned aerial vehicle.

NOMENCLATURE

		I_x, I_y, I_z	moments of inertia on x, y, z axis
		k	time variable
a	real number $0 < a$	k_l, k_p, k_q, k_r	parameters identified in [17]
b	real number $0 < b$	$k_{v1}, k_{v2}, k_{v3}, k_{v4}$	angular velocities of the propellers [rad/second], estimated in [17]
c	real number $0 < c$	m	UAV mass
c_1	constant	M_{pmodel}, M_{qmodel}	moments with respect to the x, y, z axes
D	derivative constant	M_{rmodel}	filter coefficient
$d(k)$	unmodeled dynamic	N	UAV angles for the u, v, w axis
$e(k)$	error	p, q, r	proportionality constant
F_x, F_y, F_z	forces on x, y, z axis	P	complex Laplace variable
F_{zmodel}	thrust force on the z axis	s	modulation index, pulse width modulation (PWM) signal at $[0, 1]$
g	acceleration of gravity	U_1, U_2, U_3, U_4	
g_1, g_2, g_3	constant gains		
I	integration constant		

Manuscript received April 15, 2021; revised September 8, 2021, November 4, 2021, and February 18, 2022; accepted March 21, 2022. Recommended by Associate Editor Zhijia Zhao under the direction of Editor Euntai Kim. This work was supported by the Department of Automatic Control and LAFMIA UMI of CINVESTAV-IPN, CONACYT and ITSOEH. We appreciate the support of the National Council for Science and Technology (CONACYT for its acronym in Spanish), Postdoctoral Scholarship Program, together with the Department of Automatic Control and Department of Autonomous Air and Underwater Navigation Systems of the French Mexican Laboratory of Informatics and Automatic Control, Mixed International Unit (LAFMIA UMI for its acronym in Spanish), Center for Research and Advanced Studies of the National Polytechnic Institute (CINVESTAV-IPN for its acronym in Spanish), and Electromechanical Engineering Division, Higher Technological Institute of the West of the State of Hidalgo (ITSOEH for its acronym in Spanish).

Abigail María Elena Ramírez Mendoza is with the Department of Autonomous Air and Underwater Navigation Systems, French Mexican Laboratory of Informatics and Automatic Control, Mixed International Unit (LAFMIA UMI for its acronym in Spanish), Center for Research and Advanced Studies of the National Polytechnic Institute (CINVESTAV-IPN for its acronym in Spanish). Av. Instituto Politécnico Nacional 2508, Col. San Pedro Zacatenco, C.P. 07360, México City, México. (e-mail: aramirez@cinvestav.mx). Wen Yu is with the Department of Automatic Control, CINVESTAV-IPN. Av. Instituto Politécnico Nacional 2508, Col. San Pedro Zacatenco, C.P. 07360, México City, México. (e-mail: yuw@ctrl.cinvestav.mx).

* Corresponding author.

$v_{inj}(k)$	dendrite inputs
$V_{threshold}(k)$	threshold
$w_{inj}(k)$	synaptic weights
W_c	adaptive weight
u, v, w	displacement of the UAV on u, v, w axis of the body axes
x, y, z	UAV displacement on x, y, z axis
$\tilde{y}(k)$	sigmoid activation function (SAF)
ϕ, θ, ψ	angles for rolling, pitching and yaw maneuver, at x, y, z axis
$\gamma(k)$	learning factor for unipolar systems, $0 < \gamma \leq 1$, and for bipolar systems, $-1 < \gamma \leq 1$
$\Phi(\cdot)$	a function
$\ \cdot\ $	Euclidean norm

1. INTRODUCTION

Simplified propulsion system models and algorithms have been designed for the control and navigation of multi-rotor unmanned aerial vehicle (UAV) [1,2], using various methods or approaches [3-17], to reduce the error in tracking the planned trajectory. Some of the control methods are feedback linearization-backstepping-Lyapunov function [3], proportional-integral-derivative (PID)-sliding mode control (SMC)-Lyapunov function technique and adaptive (PID-SMC-Lyapunov) [4], backpropagating-SMC-Lyapunov [5], SMC-Lyapunov [6], finite-time multiple switching SMC [7], finite-time adaptive integral backstepping fast terminal SMC [8], immersion and invariance-based SMC [9], generic adaptive SMC [10], radial basis function neural network (NN)-based adaptive distributed control [11], adaptive control [12], proportional-derivative (PD)-Lyapunov, with tunable gains [13], fuzzy-predictive controller [14], fuzzy-proportional-integral (PI) with fuzzy rules [15], adaptive neural network (ANN)-Lyapunov [16], PID-fixed gains and PID-fuzzy adaptive neurons (FAN)-self-tuning gains [17], to obtain greater precision at system response and reduce the error.

For controller design and accuracy determination in [1], they propose a survey and comparison with simulations about the most common elements included in quadrotor-vehicle models based on a typical state-space model without memory-less transformations. This new simplified model with linear internal dynamics, low complexity, and a high level of precision based on experimental data highlights the main structural features of the models to suggest particular quad-rotor vehicle control structures.

Authors of [2] describe an improved propulsion model for low-scale multi-rotor UAV, including effects of airflow speed, direction, and rotor interaction. Also, in [2], they

present two applications. The first is a propulsion envelope to determine safe operating intervals for a particular UAV, avoiding overloading the power subsystem. The second application allows to include dynamic phenomena, for instance, possible instability with closed-loop controllers.

In [3], a control scheme for tracking the trajectory of an underactuated rotary-wing vehicle is proposed. And an interconnection between translational and rotational controllers based on feedback linearization and backstepping control methods, also a Lyapunov function with the parameters of the closed-loop system controller. Numerical simulations are shown, including disturbances in attitude dynamics and noise.

An adaptive terminal sliding mode control and Lyapunov functions to ensure stability developed in [4] are used for altitude and position tracking control of quadrotor UAV with external disturbance. In addition, they present a PID-SMC-Lyapunov function technique for a known upper bound of external disturbance and an adaptive PID-SMC-Lyapunov function for an unknown upper bound of external disturbance.

A backpropagating constraints-based trajectory tracking control scheme combined with sliding-mode errors are proposed in [5], for a quadrotor. The quadrotor system consists of five cascade subsystems. A Lyapunov synthesis ensures system stability. Simulations show that trajectory tracking errors can be made arbitrarily small.

To solve precisely the trajectory-tracking problem for a marine aerial-surface heterogeneous system composed of UAV and unmanned surface vehicle, with unknown dynamics and disturbances, a coordinated trajectory tracking control scheme is created in [6]. The dynamics of system tracking errors become translation-rotation cascading manners through a family of coordinate transformations along with rotation error dynamics based on sliding mode, distributed tracking controllers, and Lyapunov analysis. Simulation results and comparisons in a prototype system demonstrate the effectiveness of the proposed scheme.

SMC is used to study the finite-time multiple switching synchronization of uncertain complex chaotic systems with network transmission mode [7], by establishing multiple switching rules.

In [8], a quadrotor UAV flight control system is presented to improve trajectory tracking performance, which combines a recursive methodology and a robust control algorithm to design a finite-time adaptive integral backstepping fast terminal SMC for position tracking and attitude stabilization, with a smooth function to attenuate chatter.

For a tilt tri-rotor UAV subject to external disturbances and unmodeled dynamics, authors of [9] propose an immersion and invariance-based SMC.

Authors of [10] provide a generic adaptive SMC for all types of UAV systems automatically or adaptively at presence of severe parametric uncertainties and unknown external disturbances.

The consensus of multiple transmission control protocol/active queue management networks is investigated using multi-agent systems in [11]. A new finite-time performance function and congestion control algorithm, NN, adaptive backstepping, a barrier Lyapunov function, and distributed control are presented to achieve output consensus and complex tasks.

To solve the Mittag-Leffler synchronization problem of fractional-order memristor NN with leakage delay, a hybrid adaptive controller that includes time delays is developed in [12].

In [13], a nonlinear hierarchical control is developed for a star-shaped hexa-rotor UAV model with tilted propellers. To solve the hovering control problem of an UAV with generically oriented propellers and intrinsically coupled translational and rotational dynamics, authors of [13] propose a control strategy, identifying the zero-moment direction and a dynamic state feedback linearization, to locally asymptotically stabilize UAV platform to a static hovering condition. A proportional-derivative (PD) and a gravity compensation feedback function tune the gains to govern the actions of the attitude transient. Methods based on Lyapunov and reduction theorems for the stability of nested sets prove stability.

Authors of [14] present a trajectory tracking solution by optimizing for multi-rotor aerial robots for a geometrically feasible trajectory, with constraints on actuators by the trajectory planner. A predictive controller model based on fuzzy logic is used to obtain a planned trajectory of the aerial robot with minimal deviation and generate the control commands for real flights at laboratory.

Tracking moving targets for quadcopters is a challenge due to complex dynamics of UAV and the variable speed of the target. A fuzzy-PI controller is developed in [15], the gains are adjusted with change of position. Fuzzy-PI controller uses two sets of PI gains and a set of fuzzy rules to achieve a nonlinear response and is compared to a gain-scheduled PID controller with fixed gains. Several experiments of an UAV are performed tracking a moving target, indoors and outdoors, day and night, with good results, especially at night.

In [16], an ANN control and optimal path planning are proposed for UAV surveillance system with energy consumption prediction. The cost function of an optimal path planning scheme, which is designed from a clustered 3D real pilot flight pattern and processed through a star and set-based particle-swarm-optimization algorithm with adaptive weights. The online ANN controller designed in [16] improves the average root-mean-square error of horizontal and vertical tracking performance. ANN controller is a method with learning ability and Lyapunov stability analysis compared to PID and fuzzy controllers, has better steady-state responses and fewer parameters to be tuned. Results show the combination of the optimal path planning scheme and the ANN controller achieves an energy-

efficient UAV surveillance system with fast disturbance rejection response.

For the identification of parameters of a simplified model of the propulsion system of a low-scale multi-rotor UAV based on experimental aerodynamic data, an efficient learning algorithm of fuzzy adaptive neurons (FAN) and a self-tuning or adaptive PID controllers for the trajectory tracking system are applied in [17]. The simulation results showed that PID controllers with FAN-self-tuning gains to track the trajectory reduce error compared to traditional PID controllers with fixed gains.

In addition, in recent years configurations for PID controllers [18-20] have been proposed, applying fuzzy logic [21-23].

Authors of [18] propose a tuning scheme for a pair of gains of a PID-type fixed parameter UAV altitude controller, with a small integral gain value. A family of methods of real-time tuning, Fibonacci-search, golden-search, equal division, and dichotomy are compared at presence of wind disturbances.

An optimal non-integer PID controller based on a deep deterministic policy gradient algorithm is presented in [19] for the tracking problem of a non-holonomic wheeled mobile robot exposed to measurement noises and external disturbances. The model-free fractional order PID (FOPID or PID) is designed, and a swarm optimization algorithm is used to set the controller parameters. Effectiveness of the control methodology is presented with the outcomes at experimental environments.

A fractional order general type-2 fuzzy PID controller is proposed in [20], to deal with the uncertainty of systems. Three-process simulations and a practical inverted pendulum system show fractional order general type-2 PID controller reduces overshoot, improves system response speed and accelerates system stability time.

Power efficiency is a motivation for designing propeller aerodynamics and optimizing the trajectory tracking of UAV, for efficient energy or fuel consumption [24].

The main contribution of this article is to develop an approximation of the FAN model [25-34], at Laplace domain to design a new fuzzy adaptive neural proportional integral derivative (FANPID) controller to track the trajectory of a low-scale UAV whose parameters were identified in [17]. The fuzzy adaptive control law (FACL) is proposed based on the FAN learning algorithm to define the gains and parameter of the FANPID controller.

Section 1 introduces the motivation, contribution and methods to solve the problem of optimizing the trajectory tracking system of the propulsion system of a low-scale UAV. Section 2 presents the preliminaries. The simplified model of low-scale UAVs and the equations of motion proposed in [17,29] are described here. The FAN model and the learning algorithm. Section 3 develops the Laplace domain approximation of FANs. Section 4 develops the design of the new FANPID-Lyapunov controller, FACL

and the stability analysis. Section 5 shows the results of the simulations and compares the error of the system obtained with PID-Fixed gains [17], PID-Fuzzy adaptive gains [17], PID-Lyapunov Function-Fixed gains [17,35], FOPID-Lyapunov-Fuzzy adaptive gains [17,19,20,35] and FANPID-Lyapunov-Fuzzy adaptive gains. And Section 6 concludes about the results of the simulations and the advantages and disadvantages of the FANPID-Lyapunov method.

2. PRELIMINARIES

2.1. Simplified model of the propulsion system of a low-scale multi-rotor UAV

Propulsion system consists of four propellers, the brushless DC rotors are operated with pulse width modulation (PWM), (1) proposed in [21] describes the dynamics of total forces and moments.

$$\begin{bmatrix} F_{zmodel} \\ M_{pmodel} \\ M_{qmodel} \\ M_{rmodel} \end{bmatrix} = \begin{bmatrix} -k_l & -k_l & -k_l & -k_l \\ k_p & -k_p & -k_p & k_p \\ k_q & k_q & -k_q & -k_q \\ -k_r & k_r & -k_r & k_r \end{bmatrix} \cdot \begin{bmatrix} (k_{v1} \cdot U_1)^2 \\ (k_{v2} \cdot U_2)^2 \\ (k_{v3} \cdot U_3)^2 \\ (k_{v4} \cdot U_4)^2 \end{bmatrix}. \quad (1)$$

Equations (2)-(7) represent the translational and rotational dynamics of the drone, based on Newton-Euler equations [27] and model proposed in [21].

$$\begin{bmatrix} \dot{x} \\ \dot{y} \\ \dot{z} \end{bmatrix} = \begin{bmatrix} \cos \psi \cos \theta & \cos \psi \sin \theta \sin \phi - \sin \psi \cos \phi \\ \sin \psi \cos \theta & \sin \psi \sin \theta \sin \phi + \cos \psi \cos \phi \\ -\sin \theta & \cos \theta \sin \phi \end{bmatrix} \cdot \begin{bmatrix} \dot{u} \\ \dot{v} \\ \dot{w} \end{bmatrix}, \quad (2)$$

$$\begin{bmatrix} \ddot{x} \\ \ddot{y} \\ \ddot{z} \end{bmatrix} = \begin{bmatrix} \frac{d\dot{x}}{dk} \\ \frac{d\dot{y}}{dk} \\ \frac{d\dot{z}}{dk} \end{bmatrix}, \quad (3)$$

$$F_x = m \cdot \ddot{x}, \quad (4)$$

$$F_y = m \cdot \ddot{y}, \quad (5)$$

$$F_z = m \cdot \ddot{z} + m \cdot g, \quad (6)$$

$$\begin{bmatrix} \dot{p} \\ \dot{q} \\ \dot{r} \end{bmatrix} = \begin{bmatrix} 1 & 0 & -\sin \theta \\ 0 & \cos \phi & \sin \phi \cos \theta \\ 0 & -\sin \phi & \cos \phi \cos \theta \end{bmatrix} \cdot \begin{bmatrix} \dot{\phi} \\ \dot{\theta} \\ \dot{\psi} \end{bmatrix}, \quad (7)$$

$$I_x \cdot \ddot{p} - (I_y - I_z) \cdot \dot{q} \cdot \dot{r} = M_{pmodel}, \quad (8)$$

$$I_y \cdot \ddot{q} + (I_x - I_z) \cdot \dot{p} \cdot \dot{r} = M_{qmodel}, \quad (9)$$

$$I_z \cdot \ddot{r} - (I_x - I_y) \cdot \dot{p} \cdot \dot{q} = M_{rmodel}, \quad (10)$$

$$\begin{bmatrix} U_1^2 \\ U_2^2 \\ U_3^2 \\ U_4^2 \end{bmatrix} = \begin{bmatrix} F_{zmodel} \\ M_{pmodel} \\ M_{qmodel} \\ M_{rmodel} \end{bmatrix} \cdot \begin{bmatrix} k_{v1}^2 \cdot (-k_l - k_l - k_l - k_l) \\ k_{v2}^2 \cdot (k_p - k_p - k_p k_p) \\ k_{v3}^2 \cdot (k_q k_q - k_q - k_q) \\ k_{v4}^2 \cdot (-k_r k_r - k_r k_r) \end{bmatrix}^{-1}. \quad (11)$$

Therefore, based on the trajectory x, y, z and the parameters identified in [17], a control system would define the drone trajectory tracking and estimate the dynamic behavior of the quadcopter UAV propulsion system. Obtaining with (11) the U_i for the rotors.

2.2. FAN model and learning algorithm

Fuzzy neurons operations are synaptic and somatic [10]. FAN model [17-26], consists of a synaptic operation (12), a Gupta-type aggregation function or fuzzy integrator (13), a nonlinear somatic operation (14)-(17), (16) for bipolar systems at $[-1, 1]$, (17) for unipolar systems at $[0, 1]$, and a learning algorithm (18)-(20) for fuzzy systems described in [20,23].

$$\tilde{V}_{min j}(k) = \min(v_{inj}(k), w_{inj}(k)), \quad (12)$$

$$\tilde{V}_{max}(k) = \text{MAX}_{j=1}^N \tilde{V}_{min j}(k), \quad (13)$$

$$\tilde{V}_{out}(k) = \max(\tilde{V}_{max}(k), V_{threshold}(k)), \quad (14)$$

$$\tilde{V}_{\gamma}(k) = \min(\gamma, \tilde{V}_{out}(k)), \quad (15)$$

$$\tilde{V}_{FAN b}(k) = \frac{2}{1 + e^{(-\tilde{V}_{\gamma}(k) \cdot c)}} - 1, \quad (16)$$

$$\tilde{V}_{FAN u}(k) = \frac{1}{1 + e^{(-\tilde{V}_{\gamma}(k) \cdot a + b)}}, \quad (17)$$

$$e(k) = \tilde{y}_{ref}(k) - \tilde{y}(k), \quad (18)$$

$$\gamma(k+1) = \gamma(k) + \Delta\gamma(k), \quad (19)$$

$$w_{inj}(k+1) = w_{inj}(k) + \Delta w_{inj}(k). \quad (20)$$

3. APPROXIMATION OF THE FAN MODEL AT DOMAIN OF LAPLACE

3.1. FAN(s)

Equation (16) describes the FAN model for bipolar systems $[-1, 1]$, with dendrite inputs $v_{inj}(k)$ and synaptic weights $w_{inj}(k)$ at time domain. Applying the Laplace transform to (16), developing the first terms of the approximation of the series, and considering the synaptic weight and $\gamma(k)$ unitary, the $V_{threshold}(k) = -1$, then

$$\mathcal{L}\{\tilde{V}_{FAN b}\} = 2 \cdot \mathcal{L}\left\{\left(1 + e^{-\tilde{V}_{\gamma}(k) \cdot c}\right)^{-1}\right\} - \mathcal{L}\{1\}, \quad (21)$$

$$\begin{aligned} \mathcal{L}\{\tilde{V}_{FAN b}\} &= 2 - \frac{2}{s+c} + \frac{2}{s+2c} - \frac{2}{s+3c} + \frac{2}{s+4c} \\ &\quad - \frac{2}{s+5c} + \frac{2}{s+6c} - \frac{2}{s+7c} + \frac{2}{s+8c} \end{aligned}$$

$$-\frac{2}{s+9c} + \frac{2}{s+10c} - \frac{1}{s}. \quad (22)$$

To obtain initial conditions equal to zero and considering $c \ll 1$, $-\frac{1}{s}$ is added,

$$\begin{aligned} \mathcal{L}\{\tilde{V}_{FAN_b}\} = & 2 - \frac{2}{s+c} + \frac{2}{s+2c} - \frac{2}{s+3c} + \frac{2}{s+4c} \\ & - \frac{2}{s+5c} + \frac{2}{s+6c} - \frac{2}{s+7c} + \frac{2}{s+8c} \\ & - \frac{2}{s+9c} + \frac{2}{s+10c} - \frac{2}{s}, \end{aligned} \quad (23)$$

$$FAN_b(s) \cong \mathcal{L}\{\tilde{V}_{FAN_b}\}. \quad (24)$$

Equation (24) is an approximation of the Laplace transform of the bipolar FAN model.

4. FANPID-LYAPUNOV CONTROLLER DESIGN, FACL AND STABILITY ANALYSIS

4.1. FANPID controller

A traditional PID controller configuration is represented by a transfer function

$$C_{PID}(s) = \left(P + I \cdot \frac{1}{s} + D \cdot \frac{N}{1 + N \cdot \frac{1}{s}} \right). \quad (25)$$

FANPID controller developed here is based on $FAN_b(s)$, transfer function is expressed in

$$\begin{aligned} C_{FANPID}(s) \\ = \left(P + I \cdot FAN_b(s) + D \cdot \frac{N}{1 + N \cdot FAN_b(s)} \right). \end{aligned} \quad (26)$$

To adjust the gains P, I, D, N and the c parameter, a FACL defined by the FAN learning algorithm is proposed.

4.2. FACL

Six $C_{FANPID}(s)$ controllers and nine FAN learning algorithms (FAN-LA) constitute the FACL for low-scale multi-rotor UAV trajectory tracking, Fig. 1.

$x_{ref}, y_{ref}, z_{ref}$ are proposed references, $\phi_{model}, \theta_{model}, \psi_{model}, P, I, D, N, c$ are obtained by the FACL, FAN-LA and FANPID controller, based on the low-scale multi-rotor UAV parameters identified in [17].

4.3. Stability analysis

Expressing the FACL in matrix form, (27) is assumed to be bounded-input-bounded-output (BIBO) stable, from Fig. 1 and (2), to obtain the models of x, y, z ,

$$\begin{bmatrix} \hat{X}(k) \\ \hat{Y}(k) \\ \hat{Z}(k) \end{bmatrix} = \int \left(\begin{bmatrix} \Sigma \Phi_x(\phi, \theta, \psi) \\ \Sigma \Phi_y(\phi, \theta, \psi) \\ \Sigma \Phi_z(\phi, \theta) \end{bmatrix} \cdot \begin{bmatrix} \dot{U} \\ \dot{V} \\ \dot{W} \end{bmatrix} \right)$$

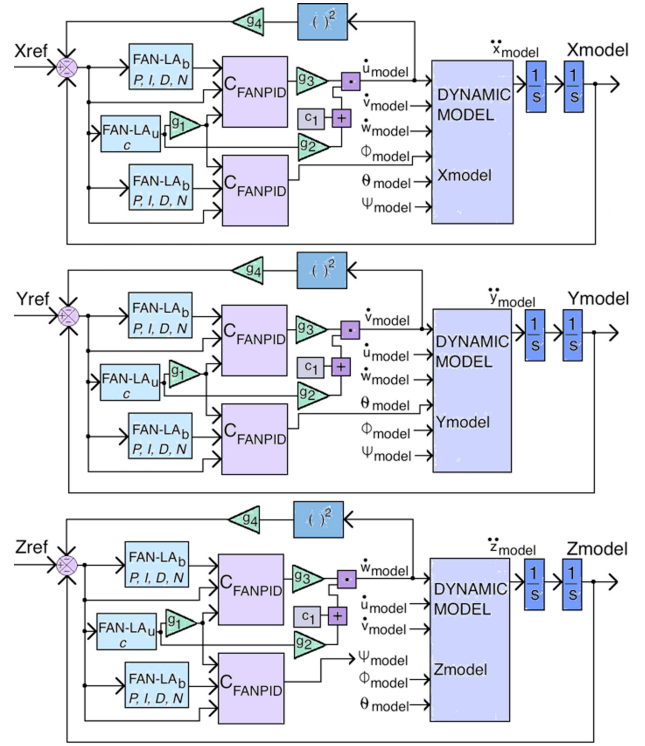


Fig. 1. Fuzzy adaptive control law.

$$\begin{aligned} & \begin{bmatrix} \Phi_{x,\phi}(C_{FANPID\phi}, C_{FANPIDx} \cdot \Phi_{1x} \cdot g_3) \\ \Phi_{y,\theta}(C_{FANPID\theta}, C_{FANPIDy} \cdot \Phi_{1y} \cdot g_3) \\ \Phi_{z,\psi}(C_{FANPID\psi}, C_{FANPIDz} \cdot \Phi_{1z} \cdot g_3) \end{bmatrix} \\ & \cdot \begin{bmatrix} W_{x,\phi} \\ W_{y,\theta} \\ W_{z,\psi} \end{bmatrix}, \end{aligned} \quad (27)$$

where

$$\Phi_1 = W_c \cdot g_2 + c_1,$$

$$C_{FANPID} = \Phi_{PID}(\Phi_{FAN_b}(W_c \cdot g_1)),$$

$$W_{x,\phi} = [W_{Px}, W_{Ix}, W_{Dx}, W_{Nx}, W_{P\phi}, W_{I\phi}, W_{D\phi}, W_{N\phi}],$$

$$W_{y,\theta} = [W_{Py}, W_{Iy}, W_{Dy}, W_{Ny}, W_{P\theta}, W_{I\theta}, W_{D\theta}, W_{N\theta}],$$

$$W_{z,\psi} = [W_{Pz}, W_{Iz}, W_{Dz}, W_{Nz}, W_{P\psi}, W_{I\psi}, W_{D\psi}, W_{N\psi}].$$

Adaptive sliding surfaces are

$$\begin{bmatrix} s_{x,\phi} \\ s_{y,\theta} \\ s_{z,\psi} \end{bmatrix} = \begin{bmatrix} \Phi_{x,\phi}(C_{FANPID\phi}, C_{FANPIDx} \cdot \Phi_{1x} \cdot g_3) \\ \Phi_{y,\theta}(C_{FANPID\theta}, C_{FANPIDy} \cdot \Phi_{1y} \cdot g_3) \\ \Phi_{z,\psi}(C_{FANPID\psi}, C_{FANPIDz} \cdot \Phi_{1z} \cdot g_3) \end{bmatrix} \cdot \begin{bmatrix} W_{x,\phi} \\ W_{y,\theta} \\ W_{z,\psi} \end{bmatrix}.$$

Then, the model (27) considering the unmodeled dynamics would be

$$\begin{aligned}
 \begin{bmatrix} X(k) \\ Y(k) \\ Z(k) \end{bmatrix} &= \int \left(\begin{bmatrix} \sum \Phi_x(\phi, \theta, \psi) \\ \sum \Phi_y(\phi, \theta, \psi) \\ \sum \Phi_z(\phi, \theta) \end{bmatrix} \cdot \begin{bmatrix} \dot{U} \\ \dot{V} \\ \dot{W} \end{bmatrix} \right. \\
 &\quad \cdot \begin{bmatrix} \Phi_{x,\phi}(C_{FANPID\phi}, C_{FANPIDx} \cdot \Phi_{1x} \cdot g_3) \\ \Phi_{y,\theta}(C_{FANPID\theta}, C_{FANPIDy} \cdot \Phi_{1y} \cdot g_3) \\ \Phi_{z,\psi}(C_{FANPID\psi}, C_{FANPIDz} \cdot \Phi_{1z} \cdot g_3) \\ \left. \begin{bmatrix} W_{x,\phi}^* \\ W_{y,\theta}^* \\ W_{z,\psi}^* \end{bmatrix} \right) \\
 &+ \int \left(\begin{bmatrix} \sum \Phi_x(\phi_d, \theta_d, \psi_d) \\ \sum \Phi_y(\phi_d, \theta_d, \psi_d) \\ \sum \Phi_z(\phi_d, \theta_d) \end{bmatrix} \cdot \begin{bmatrix} \dot{U}_d \\ \dot{V}_d \\ \dot{W}_d \end{bmatrix} \right. \\
 &\quad \cdot \begin{bmatrix} \Phi_{x_d,\phi_d}(C_{FANPID\phi_d}, C_{FANPIDx_d} \cdot \Phi_{1x_d} \cdot g_3) \\ \Phi_{y_d,\theta_d}(C_{FANPID\theta_d}, C_{FANPIDy_d} \cdot \Phi_{1y_d} \cdot g_3) \\ \Phi_{z_d,\psi_d}(C_{FANPID\psi_d}, C_{FANPIDz_d} \cdot \Phi_{1z_d} \cdot g_3) \\ \left. \begin{bmatrix} W_{x,\phi_d}^* \\ W_{y,\theta_d}^* \\ W_{z,\psi_d}^* \end{bmatrix} \right) + d(k), \quad (28)
 \end{aligned}$$

where

$$\begin{aligned}
 W_{x,\phi_d}^* &= [W_{Px_d}, W_{Ix_d}, W_{Dx_d}, W_{Nx_d}, W_{P\phi_d}, W_{I\phi_d}, \\
 &\quad W_{D\phi_d}, W_{N\phi_d}], \\
 W_{y,\theta_d}^* &= [W_{Py_d}, W_{Iy_d}, W_{Dy_d}, W_{Ny_d}, W_{P\theta_d}, W_{I\theta_d}, \\
 &\quad W_{D\theta_d}, W_{N\theta_d}], \\
 W_{z,\psi_d}^* &= [W_{Pz_d}, W_{Iz_d}, W_{Dz_d}, W_{Nz_d}, W_{P\psi_d}, W_{I\psi_d}, \\
 &\quad W_{D\psi_d}, W_{N\psi_d}],
 \end{aligned}$$

W_{x,ϕ_d}^* , W_{y,θ_d}^* , W_{z,ψ_d}^* are unknown weights to minimize the unmodeled dynamic,

$$\begin{aligned}
 \int \left(\begin{bmatrix} \sum \Phi_x(\phi_d, \theta_d, \psi_d) \\ \sum \Phi_y(\phi_d, \theta_d, \psi_d) \\ \sum \Phi_z(\phi_d, \theta_d) \end{bmatrix} \cdot \begin{bmatrix} \dot{U}_d \\ \dot{V}_d \\ \dot{W}_d \end{bmatrix} \right. \\
 \cdot \begin{bmatrix} \Phi_{x_d,\phi_d}(C_{FANPID\phi_d}, C_{FANPIDx_d} \cdot \Phi_{1x_d} \cdot g_3) \\ \Phi_{y_d,\theta_d}(C_{FANPID\theta_d}, C_{FANPIDy_d} \cdot \Phi_{1y_d} \cdot g_3) \\ \Phi_{z_d,\psi_d}(C_{FANPID\psi_d}, C_{FANPIDz_d} \cdot \Phi_{1z_d} \cdot g_3) \\ \left. \begin{bmatrix} W_{x,\phi_d}^* \\ W_{y,\theta_d}^* \\ W_{z,\psi_d}^* \end{bmatrix} \right) \cdot
 \end{aligned}$$

FACL trajectory tracking error is defined with the FAN method in matrix form

$$\begin{bmatrix} E_x(k) \\ E_y(k) \\ E_z(k) \end{bmatrix} = \begin{bmatrix} X(k) \\ Y(k) \\ Z(k) \end{bmatrix} - \begin{bmatrix} \hat{X}(k) \\ \hat{Y}(k) \\ \hat{Z}(k) \end{bmatrix} - \begin{bmatrix} g_4 \cdot \Phi_u(\dot{U}) \\ g_4 \cdot \Phi_v(\dot{V}) \\ g_4 \cdot \Phi_w(\dot{W}) \end{bmatrix}, \quad (29)$$

$$\begin{aligned}
 \begin{bmatrix} E_x(k) \\ E_y(k) \\ E_z(k) \end{bmatrix} &\cong \int \left(\begin{bmatrix} \int \Phi_x(\phi, \theta, \psi) \\ \int \Phi_y(\phi, \theta, \psi) \\ \int \Phi_z(\phi, \theta) \end{bmatrix} \cdot \begin{bmatrix} \dot{U} \\ \dot{V} \\ \dot{W} \end{bmatrix} \right. \\
 &\quad \cdot \begin{bmatrix} \Phi_{x,\phi}(C_{FANPID\phi}, C_{FANPIDx} \cdot \Phi_{1x} \cdot g_3) \\ \Phi_{y,\theta}(C_{FANPID\theta}, C_{FANPIDy} \cdot \Phi_{1y} \cdot g_3) \\ \Phi_{z,\psi}(C_{FANPID\psi}, C_{FANPIDz} \cdot \Phi_{1z} \cdot g_3) \\ \left. \begin{bmatrix} \tilde{W}_{x,\phi} \\ \tilde{W}_{y,\theta} \\ \tilde{W}_{z,\psi} \end{bmatrix} \right) \\
 &+ \int \left(\begin{bmatrix} \int \Phi_x(\phi_d, \theta_d, \psi_d) \\ \int \Phi_y(\phi_d, \theta_d, \psi_d) \\ \int \Phi_z(\phi_d, \theta_d) \end{bmatrix} \cdot \begin{bmatrix} \dot{U}_d \\ \dot{V}_d \\ \dot{W}_d \end{bmatrix} \right. \\
 &\quad \cdot \begin{bmatrix} \Phi_{x_d,\phi_d}(C_{FANPID\phi_d}, C_{FANPIDx_d} \cdot \Phi_{1x_d} \cdot g_3) \\ \Phi_{y_d,\theta_d}(C_{FANPID\theta_d}, C_{FANPIDy_d} \cdot \Phi_{1y_d} \cdot g_3) \\ \Phi_{z_d,\psi_d}(C_{FANPID\psi_d}, C_{FANPIDz_d} \cdot \Phi_{1z_d} \cdot g_3) \\ \left. \begin{bmatrix} W_{x,\phi_d}^* \\ W_{y,\theta_d}^* \\ W_{z,\psi_d}^* \end{bmatrix} \right) - \begin{bmatrix} g_4 \cdot \Phi_u(\dot{U}) \\ g_4 \cdot \Phi_v(\dot{V}) \\ g_4 \cdot \Phi_w(\dot{W}) \end{bmatrix}, \quad (30)
 \end{aligned}$$

$$\begin{aligned}
 \begin{bmatrix} E_x(k) \\ E_y(k) \\ E_z(k) \end{bmatrix} &\cong \int \left(\begin{bmatrix} \int \Phi_x(\phi, \theta, \psi) \\ \int \Phi_y(\phi, \theta, \psi) \\ \int \Phi_z(\phi, \theta) \end{bmatrix} \cdot \begin{bmatrix} \dot{U} \\ \dot{V} \\ \dot{W} \end{bmatrix} \right. \\
 &\quad \cdot \begin{bmatrix} \Phi_{x,\phi}(C_{FANPID\phi}, C_{FANPIDx} \cdot \Phi_{1x} \cdot g_3) \\ \Phi_{y,\theta}(C_{FANPID\theta}, C_{FANPIDy} \cdot \Phi_{1y} \cdot g_3) \\ \Phi_{z,\psi}(C_{FANPID\psi}, C_{FANPIDz} \cdot \Phi_{1z} \cdot g_3) \\ \left. \begin{bmatrix} \tilde{W}_{x,\phi} \\ \tilde{W}_{y,\theta} \\ \tilde{W}_{z,\psi} \end{bmatrix} \right) + \mu_d - \eta_d, \quad (31)
 \end{aligned}$$

where

$$\begin{bmatrix} \tilde{W}_{x,\phi} \\ \tilde{W}_{y,\theta} \\ \tilde{W}_{z,\psi} \end{bmatrix} = \begin{bmatrix} W_{x,\phi}^* \\ W_{y,\theta}^* \\ W_{z,\psi}^* \end{bmatrix} - \begin{bmatrix} W_{x,\phi} \\ W_{y,\theta} \\ W_{z,\psi} \end{bmatrix},$$

$$\mu_d = \int \left(\begin{bmatrix} \int \Phi_x(\phi_d, \theta_d, \psi_d) \\ \int \Phi_y(\phi_d, \theta_d, \psi_d) \\ \int \Phi_z(\phi_d, \theta_d) \end{bmatrix} \cdot \begin{bmatrix} \dot{U}_d \\ \dot{V}_d \\ \dot{W}_d \end{bmatrix} \right)$$

$$\eta_d = \begin{pmatrix} \begin{bmatrix} \Phi_{x_d, \phi_d}(C_{FANPID\phi_d}, C_{FANPIDx_d} \cdot \Phi_{1x_d} \cdot g_3) \\ \Phi_{y_d, \theta_d}(C_{FANPID\theta_d}, C_{FANPIDy_d} \cdot \Phi_{1y_d} \cdot g_3) \\ \Phi_{z_d, \psi_d}(C_{FANPID\psi_d}, C_{FANPIDz_d} \cdot \Phi_{1z_d} \cdot g_3) \end{bmatrix} \cdot \begin{bmatrix} W_{x, \phi_d}^* \\ W_{y, \theta_d}^* \\ W_{z, \psi_d}^* \end{bmatrix} \\ g_4 \cdot \Phi_u(\dot{U}) \\ g_4 \cdot \Phi_v(\dot{V}) \\ g_4 \cdot \Phi_w(\dot{W}) \end{pmatrix},$$

where $\Phi_u(\cdot) = \Phi_v(\cdot) = \Phi_w(\cdot) = (\cdot)^2$ is a Lyapunov function candidate.

FAN-LA described in [18] is presented below

$$W(k+1) = W(k) + \Gamma(k) \cdot E(k) \cdot D(k), \quad (32)$$

$$\Gamma(k+1) = \Gamma(k) + \Gamma(k) \cdot E(k) \cdot D(k). \quad (33)$$

For the closed-loop multi-rotor UAV trajectory tracking system, the FACL model (27) is assumed to be stable bounded-input-bounded-output (BIBO). FAN-LA and $W_{x, \phi}$, $W_{y, \theta}$, $W_{z, \psi}$ weights are bounded at $[0, 1]$ for unipolar and at $[-1, 1]$ for bipolar. Stability analysis for modeling nonlinear closed-loop systems based on the new FAN method is stated by the following theorem.

Theorem 1: If the unknown closed-loop nonlinear system Fig. 1, is modeled by the fuzzy system (27), the weights are updated by (32) and (33), then the modeling error $E(k) = [E_x(k), E_y(k), E_z(k)]^T$ is uniformly ultimately bounded (UUB). The normalized identification error is

$$E_N(k) = \frac{W_N(k+1) - W_N(k)}{\Gamma_N(k) \cdot D(k)}. \quad (34)$$

Satisfying the average performance

$$\begin{aligned} & \limsup_{T \rightarrow \infty} \frac{1}{T} \sum_{k=1}^T \|E_N(k)\|^2 \\ & \leq \max_k \left\| \int \begin{pmatrix} \int \Phi_x(\phi_d, \theta_d, \psi_d) \\ \int \Phi_y(\phi_d, \theta_d, \psi_d) \\ \int \Phi_z(\phi_d, \theta_d) \end{pmatrix} \cdot \begin{bmatrix} \dot{U}_d \\ \dot{V}_d \\ \dot{W}_d \end{bmatrix} \right\| \\ & \cdot \left\| \begin{bmatrix} \Phi_{x_d, \phi_d}(C_{FANPID\phi_d}, C_{FANPIDx_d} \cdot \Phi_{1x_d} \cdot g_3) \\ \Phi_{y_d, \theta_d}(C_{FANPID\theta_d}, C_{FANPIDy_d} \cdot \Phi_{1y_d} \cdot g_3) \\ \Phi_{z_d, \psi_d}(C_{FANPID\psi_d}, C_{FANPIDz_d} \cdot \Phi_{1z_d} \cdot g_3) \end{bmatrix} \cdot \begin{bmatrix} W_{x, \phi_d}^* \\ W_{y, \theta_d}^* \\ W_{z, \psi_d}^* \end{bmatrix} \right\|^2, \\ & \limsup_{T \rightarrow \infty} \frac{1}{T} \sum_{k=1}^T \|E_N(k)\|^2 \leq \bar{\mu}_d. \end{aligned} \quad (35)$$

Proof: A defined positive scalar L_k is selected

$$L_k = \|\tilde{W}(k)\|^2, \quad (36)$$

where

$$\tilde{W}(k) = [\tilde{W}_{x, \phi}(k), \tilde{W}_{y, \theta}(k), \tilde{W}_{z, \psi}(k)]^T.$$

By the update law (32), we have

$$\tilde{W}(k+1) = \tilde{W}(k) + \Gamma(k) \cdot E(k) \cdot D(k). \quad (37)$$

Using the inequalities

$$\|q+r\| \leq \|q\| + \|r\|, \quad \|q \cdot r\| = \|q\| \cdot \|r\|.$$

For any “ q ” and “ r ”, and using (31) and (37) with $-1 < \Gamma_N(k) \leq \Gamma(k) \leq 1$, we have

$$\begin{aligned} \Delta L_k & = L_{k+1} - L_k \\ & = \|\tilde{W}(k) + \Gamma(k) \cdot E(k) \cdot D(k)\|^2 - \|\tilde{W}(k)\|^2 \\ & = 2\|\Gamma(k) \cdot E(k) \cdot D(k) \cdot \tilde{W}(k)\| + \|\Gamma(k) \cdot E(k) \cdot D(k)\|^2 \\ & = \|\Gamma(k)\|^2 \cdot \|E(k)\|^2 \cdot \|D(k)\|^2 \\ & + 2 \left\| \begin{pmatrix} \Gamma(k) \cdot E(k) \cdot D(k) \cdot \frac{d(E(k) - \mu_d + \eta_d)}{dk} \\ \begin{bmatrix} \Sigma \Phi_x(\phi, \theta, \psi) \\ \Sigma \Phi_y(\phi, \theta, \psi) \\ \Sigma \Phi_z(\phi, \theta) \end{bmatrix} \cdot \begin{bmatrix} \dot{U} \\ \dot{V} \\ \dot{W} \end{bmatrix} \\ \begin{bmatrix} \Phi_{x, \phi}(C_{FANPID\phi}, C_{FANPIDx} \cdot \Phi_{1x} \cdot g_3) \\ \Phi_{y, \theta}(C_{FANPID\theta}, C_{FANPIDy} \cdot \Phi_{1y} \cdot g_3) \\ \Phi_{z, \psi}(C_{FANPID\psi}, C_{FANPIDz} \cdot \Phi_{1z} \cdot g_3) \end{bmatrix} \end{pmatrix} \right\|, \end{aligned} \quad (38)$$

$$\begin{aligned} \Delta L_k & \leq \zeta(k) \cdot \|E(k)\|^2 + \delta(k) \cdot \|E(k)\| \cdot \|\dot{E}(k)\| \\ & + \rho(k) \cdot \|E(k)\|, \end{aligned} \quad (39)$$

where $\zeta(k)$, $\delta(k)$ and $\rho(k)$ are defined

$$\begin{aligned} \zeta(k) & = \|\Gamma(k)\|^2 \cdot \|D(k)\|^2, \\ \delta(k) & = 2 \left\| \begin{pmatrix} \Gamma(k) \cdot D(k) \\ \begin{bmatrix} \Sigma \Phi_x(\phi, \theta, \psi) \\ \Sigma \Phi_y(\phi, \theta, \psi) \\ \Sigma \Phi_z(\phi, \theta) \end{bmatrix} \cdot \begin{bmatrix} \dot{U} \\ \dot{V} \\ \dot{W} \end{bmatrix} \\ \begin{bmatrix} \Phi_{x, \phi}(C_{FANPID\phi}, C_{FANPIDx} \cdot \Phi_{1x} \cdot g_3) \\ \Phi_{y, \theta}(C_{FANPID\theta}, C_{FANPIDy} \cdot \Phi_{1y} \cdot g_3) \\ \Phi_{z, \psi}(C_{FANPID\psi}, C_{FANPIDz} \cdot \Phi_{1z} \cdot g_3) \end{bmatrix} \end{pmatrix} \right\|, \\ \rho(k) & \end{aligned}$$

$$= 2 \left\| \left(\begin{array}{c} \Gamma(k) \cdot D(k) \cdot (-\dot{\mu}_d + \dot{\eta}_d) \\ \left[\begin{array}{c} \sum \Phi_x(\phi, \theta, \psi) \\ \sum \Phi_y(\phi, \theta, \psi) \\ \sum \Phi_z(\phi, \theta) \end{array} \right] \cdot \left[\begin{array}{c} \dot{U} \\ \dot{V} \\ \dot{W} \end{array} \right] \\ \Phi_{x,\phi}(C_{FANPID\phi}, C_{FANPIDx} \Phi_{1x} \cdot g_3) \\ \Phi_{y,\theta}(C_{FANPID\theta}, C_{FANPIDy} \Phi_{1y} \cdot g_3) \\ \Phi_{z,\psi}(C_{FANPID\psi}, C_{FANPIDz} \Phi_{1z} \cdot g_3) \end{array} \right) \right\|.$$

Because

$$n \min(\tilde{w}_i^2) \leq L_k \leq n \max(\tilde{w}_i^2),$$

where $n \min(\tilde{w}_i^2)$ and $n \max(\tilde{w}_i^2)$ are \mathcal{K}_∞ -functions, and $\zeta(k) \cdot \|E(k)\|^2$, $\delta(k) \cdot \|E(k)\| \cdot \|\dot{E}(k)\|$, $\rho(k) \cdot \|E(k)\|$ are a \mathcal{K}_∞ -function. So, L_k admits an ISS-Lyapunov function [23], the dynamic of the identification error is input-to-state stable.

From (28) and (36) we know that L_k is the function of $E(k)$ and

$$\int \left(\begin{array}{c} \left[\begin{array}{c} \sum \Phi_x(\phi_d, \theta_d, \psi_d) \\ \sum \Phi_y(\phi_d, \theta_d, \psi_d) \\ \sum \Phi_z(\phi_d, \theta_d) \end{array} \right] \cdot \left[\begin{array}{c} \dot{U}_d \\ \dot{V}_d \\ \dot{W}_d \end{array} \right] \\ \Phi_{x_d, \phi_d}(C_{FANPID\phi_d}, C_{FANPIDx_d} \Phi_{1x_d} \cdot g_3) \\ \Phi_{y_d, \theta_d}(C_{FANPID\theta_d}, C_{FANPIDy_d} \Phi_{1y_d} \cdot g_3) \\ \Phi_{z_d, \psi_d}(C_{FANPID\psi_d}, C_{FANPIDz_d} \Phi_{1z_d} \cdot g_3) \\ \left[\begin{array}{c} W_{x,\phi d}^* \\ W_{y,\theta d}^* \\ W_{z,\psi d}^* \end{array} \right] \end{array} \right).$$

The ‘‘INPUT’’ and the ‘‘STATE’’ correspond to both terms of (27). However, usually, $\Phi[\phi_d, \theta_d, \psi_d] \ll \Phi[\phi, \theta, \psi]$. Because the ‘‘INPUT’’ is bounded and the dynamic is ISS, therefore the ‘‘STATE’’ $E(k)$ is bounded.

Applying the bounded conditions for $W_N(k+1)$ and $\Gamma_N(k+1)$, (39), from 1 up to T and using $0 < L_T$ and L_1 is a constant, we obtain

$$\begin{aligned} L_T - L_1 &\leq \zeta_N(k) \cdot \left(\sum_{k=1}^T \|E_N(k)\|^2 \right) \\ &\quad + \delta_N(k) \cdot \left(\sum_{k=1}^T \|E_N(k)\| \cdot \|\dot{E}_N(k)\| \right) \\ &\quad + \rho_N(k) \cdot \left(\sum_{k=1}^T \|E_N(k)\| \right), \end{aligned} \quad (40)$$

$$\zeta_N(k) = \|\Gamma_N(k)\|^2 \cdot \|D(k)\|^2,$$

$$\delta_N(k)$$

$$= 2 \left\| \left(\begin{array}{c} \Gamma_N(k) \cdot D(k) \\ \left[\begin{array}{c} \sum \Phi_x(\phi, \theta, \psi) \\ \sum \Phi_y(\phi, \theta, \psi) \\ \sum \Phi_z(\phi, \theta) \end{array} \right] \cdot \left[\begin{array}{c} \dot{U} \\ \dot{V} \\ \dot{W} \end{array} \right] \\ \Phi_{x,\phi}(C_{FANPID\phi}, C_{FANPIDx} \Phi_{1x} \cdot g_3) \\ \Phi_{y,\theta}(C_{FANPID\theta}, C_{FANPIDy} \Phi_{1y} \cdot g_3) \\ \Phi_{z,\psi}(C_{FANPID\psi}, C_{FANPIDz} \Phi_{1z} \cdot g_3) \end{array} \right) \right\|,$$

$$\rho_N(k)$$

$$= 2 \left\| \left(\begin{array}{c} \Gamma_N(k) \cdot D(k) \cdot (-\dot{\mu}_d + \dot{\eta}_d) \\ \left[\begin{array}{c} \sum \Phi_x(\phi, \theta, \psi) \\ \sum \Phi_y(\phi, \theta, \psi) \\ \sum \Phi_z(\phi, \theta) \end{array} \right] \cdot \left[\begin{array}{c} \dot{U} \\ \dot{V} \\ \dot{W} \end{array} \right] \\ \Phi_{x,\phi}(C_{FANPID\phi}, C_{FANPIDx} \Phi_{1x} \cdot g_3) \\ \Phi_{y,\theta}(C_{FANPID\theta}, C_{FANPIDy} \Phi_{1y} \cdot g_3) \\ \Phi_{z,\psi}(C_{FANPID\psi}, C_{FANPIDz} \Phi_{1z} \cdot g_3) \end{array} \right) \right\|,$$

$$\begin{aligned} L_T - L_1 - \rho_N(k) \cdot \left(\sum_{k=1}^T \|E_N(k)\| \right) \\ \leq \zeta_N(k) \cdot \left(\sum_{k=1}^T \|E_N(k)\|^2 \right) \\ + \delta_N(k) \cdot \left(\sum_{k=1}^T \|E_N(k)\| \cdot \|\dot{E}_N(k)\| \right). \end{aligned} \quad (41)$$

Equation (35) is established. \square

Remark 1: To obtain high modeling accuracy for traditional PID controllers, the main difficulty is to adjust the gains. However, the novel configuration of the FANPID-Lyapunov controller with FAN-LA to tune the gains has fewer parameters to choose from. And the modeling error converges to the zone $\bar{\mu}_d$.

Remark 2: If the fuzzy system (27) could exactly match the nonlinear plant (28), if $\mu_d(k) = 0$, i.e., it could find the best W^* such that the nonlinear system could be expressed as

$$\begin{aligned} \begin{bmatrix} X(k) \\ Y(k) \\ Z(k) \end{bmatrix} &= \sum \left(\begin{array}{c} \left[\begin{array}{c} f \Phi_x(\phi, \theta, \psi) \\ f \Phi_y(\phi, \theta, \psi) \\ f \Phi_z(\phi, \theta) \end{array} \right] \cdot \left[\begin{array}{c} \dot{U} \\ \dot{V} \\ \dot{W} \end{array} \right] \\ \Phi_{x,\phi}(C_{FANPID\phi}, C_{FANPIDx} \Phi_{1x} \cdot g_3) \\ \Phi_{y,\theta}(C_{FANPID\theta}, C_{FANPIDy} \Phi_{1y} \cdot g_3) \\ \Phi_{z,\psi}(C_{FANPID\psi}, C_{FANPIDz} \Phi_{1z} \cdot g_3) \\ \left[\begin{array}{c} W_{x,\phi d}^* \\ W_{y,\theta d}^* \\ W_{z,\psi d}^* \end{array} \right] \end{array} \right), \end{aligned}$$

the same learning law makes the error identified $\|E(k)\|$

asymptotically stable

$$\lim_{K \rightarrow \infty} \|E(k)\| = 0. \quad (42)$$

Remark 3: The normalization of learning rates in (43) and (47), are time-varying to ensure the stability of identification error. Learning rates are easier to achieve than [17]. Because the initial condition does not need any previous information, the time-varying learning rates and the FACL are optimized.

5. SIMULATION RESULTS

5.1. Initial conditions

Figs. 2-9 present the simulation results of the FACL (27) and the closed-loop multi-rotor UAV trajectory tracking system in Matlab[®]/Simulink. The fuzzy adaptive system Fig. 1, consists of six FANPID controllers, three Lyapunov functions, and nine FAN-LA to tune the gains and parameter c of the FAN(s) model. The initial conditions are

- 1) Weights, $w_{inFAN-LA_{ip}}(k) = 1$, $w_{inFAN-LA_{il}}(k) = 0.6$, $w_{inFAN-LA_{id}}(k) = 0.1$, $w_{inFAN-LA_{in}}(k) = 0.2$, $w_{inFAN-LA_{ic}}(k) = 0$, $i = x, y, z$.
- 2) Learning factors, fixed values, $\gamma_{FAN_i}(k) = 1$.
- 3) The threshold values for all the FANs are

$$V_{threshold1FAN_i}(k) = -1.$$

- 4) FAN-LA inputs, $D_{FAN_{ij}}(k) = D_{FAN_{nc}}(k) = 1$, $i = 1, \dots, 6$, $j = P, I, D, N$, $n = 1, \dots, 3$.
- 5) Reference outputs

$$XYZ_{ref}(k) = [X_{ref}(k), Y_{ref}(k), Z_{ref}(k)]^T.$$

- 6) Ideal values of weights are unknown.
- 7) $g_1 = 700$, $g_2 = 4e - 7$, $g_3 = 1e - 6$.
- 8) Sampling period is $K_{sample} = 1e - 3$ seconds.

5.2. Results of the multi-rotor UAV tracking trajectory system

$X_{ref}(k)$, $Y_{ref}(k)$, $Z_{ref}(k)$ are the position references, Fig. 2 shows the tracking trajectory obtained from model (27). Fig. 3 presents the angles modeled $\phi_{model}(k)$, $\theta_{model}(k)$, $\psi_{model}(k)$ by the fuzzy adaptive system. The three-dimensional reference and modeled trajectory are shown in Fig. 4.

Fig. 5 compares the error (48) obtained of a PID-Fixed weights [17], a PID-Fuzzy adaptive weights [17], a PID-Lyapunov-Fixed weights [17,35], (43), (44), FOPID-Lyapunov-FAN-LA-Self-tuning gains and parameters [19, 20], $C_{FOPID}(s) = (P + I \cdot \frac{1}{s} + \frac{D \cdot s^d}{n \cdot s^d + 1})$, $n \in \mathbb{R}$, η_d , (43), (44), with the proposed references $x, y, z, \phi, \theta, \psi$, and the new FANPID-Lyapunov-Self-tuning gains and parameter (26), with the proposed references x, y, z , and ϕ, θ, ψ adaptive,

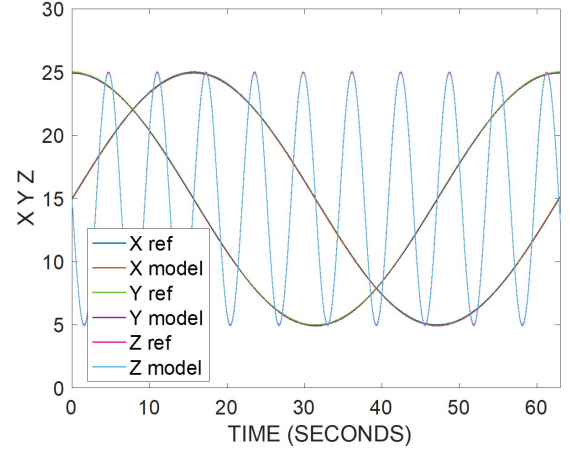


Fig. 2. $X_{ref}, Y_{ref}, Z_{ref}, X_{model}, Y_{model}, Z_{model}$ for tracking the trajectory of the multi-rotor UAV.

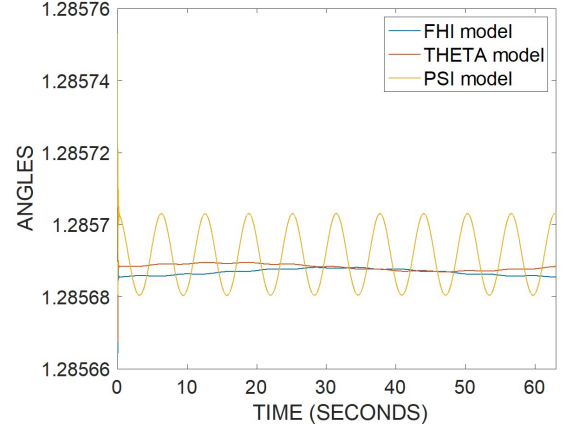


Fig. 3. $\phi_{model}, \theta_{model}, \psi_{model}$ for tracking the trajectory of the multi-rotor UAV.

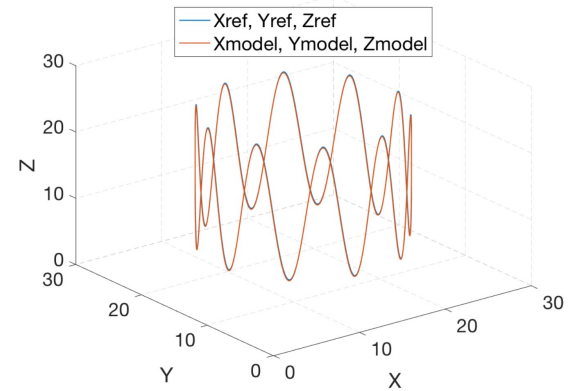
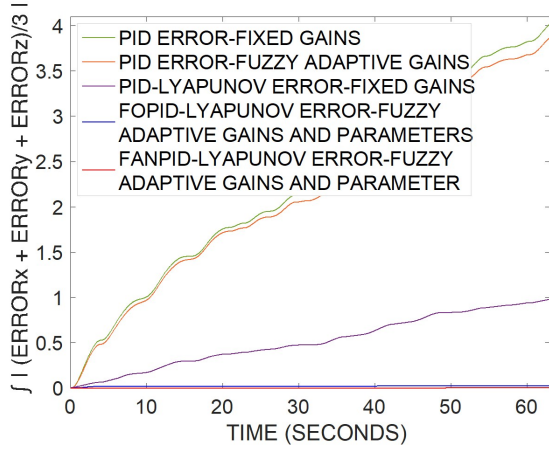


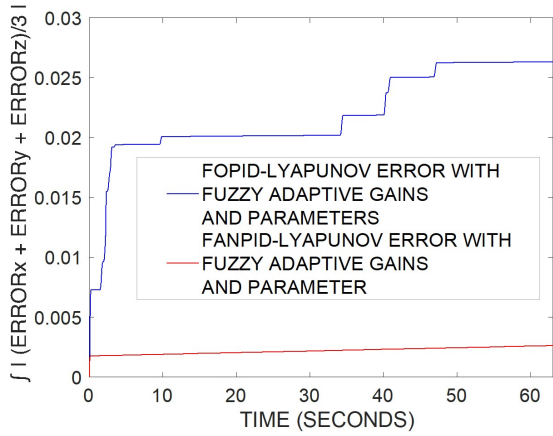
Fig. 4. $X_{ref}, Y_{ref}, Z_{ref}, X_{model}, Y_{model}, Z_{model}$ for tracking the trajectory of the multi-rotor UAV.

further reducing error and verifying the superiority of the method.

Lyapunov function $V_{x,y,z}$, for PID-Lyapunov-Fixed



(a)



(b)

Fig. 5. (a) Error of the fixed-gains PID, self-tuning PID, fixed-gains PID-Lyapunov, self-tuning FOPID-Lyapunov and self-tuning FANPID-Lyapunov of FACL system. (b) Self-tuning FOPID-Lyapunov and self-tuning FANPID-Lyapunov.

weights controller is defined in

$$\begin{bmatrix} V_x(X) \\ V_y(Y) \\ V_z(Z) \end{bmatrix} = \beta \cdot \begin{bmatrix} (X(k) - \hat{X}(k))^2 \\ (Y(k) - \hat{Y}(k))^2 \\ (Z(k) - \hat{Z}(k))^2 \end{bmatrix} \cdot \begin{bmatrix} \text{sign}_x(X(k) - \hat{X}(k)) \\ \text{sign}_y(Y(k) - \hat{Y}(k)) \\ \text{sign}_z(Z(k) - \hat{Z}(k)) \end{bmatrix}, \quad (43)$$

where β is a constant.

$$\text{sign}_{x,y,z}(\cdot) = \begin{cases} 1, & \text{if } (\cdot) > 0, \\ 0, & \text{if } (\cdot) = 0, \\ -1, & \text{if } (\cdot) < 0. \end{cases} \quad (44)$$

Theorem 2: Let $[X, Y, Z]^T = [X_0, Y_0, Z_0]^T$ an equilibrium point for (27), and let $[V_x(X), V_y(Y), V_z(Z)]^T : \mathcal{R}^n \rightarrow \mathcal{R}$ a continuously differentiable function such that

$$\begin{aligned} [V_x(X_0), V_y(Y_0), V_z(Z_0)]^T &= [X_0, Y_0, Z_0]^T \text{ and} \\ [V_x(X), V_y(Y), V_z(Z)]^T &> [X_0, Y_0, Z_0]^T, \\ \forall [X, Y, Z]^T &\neq [X_0, Y_0, Z_0]^T, \end{aligned} \quad (45)$$

$$\begin{aligned} [\|X\|, \|Y\|, \|Z\|]^T \rightarrow \infty &\Rightarrow [V_x(X), V_y(Y), V_z(Z)]^T \\ &\rightarrow \infty, \end{aligned} \quad (46)$$

$$\begin{aligned} [\dot{V}_x(X), \dot{V}_y(Y), \dot{V}_z(Z)]^T &< [X_0, Y_0, Z_0]^T, \\ \forall [X, Y, Z]^T &\neq [X_0, Y_0, Z_0]^T. \end{aligned} \quad (47)$$

Then, $[X, Y, Z]^T = [X_0, Y_0, Z_0]^T$ is globally asymptotically stable.

$$\begin{aligned} E_{PID-FANself-tuning}(k) \\ = \int \left| \frac{E_xPID-FAN(k) + E_yPID-FAN(k) + E_zPID-FAN(k)}{3} \right|. \end{aligned} \quad (48)$$

$F_{Zmodel}, M_{pmodel}, M_{qmodel}, M_{rmodel}$ forces and moments, and modulation indices $U_{1model}, U_{2model}, U_{3model}, U_{4model}$ are shown in Figs. 6-9.

Remark 4: From Fig. 5, the self-adjusting FOPID-Lyapunov applies the FAN-LA, proposing the constant n , the adaptive parameters P, I, D , and with $\lambda = \mu$, thus further reducing the error.

Remark 5: FAN-LA self-tunes the P, I, D, N, c parameters of FANPID-Lyapunov optimizing the response of FACL system, significantly reducing error. FANPID-Lyapunov method and the FACL adapt the FANPID parameters for the simplified model of the propulsion system of a low-scale multi-rotor UAV.

Fig. 3 shows that applying the FACL the multi-rotor UAV tracks the trajectory and tunes $\phi_{model}, \theta_{model}, \psi_{model}$, Fig. 4, with great success.

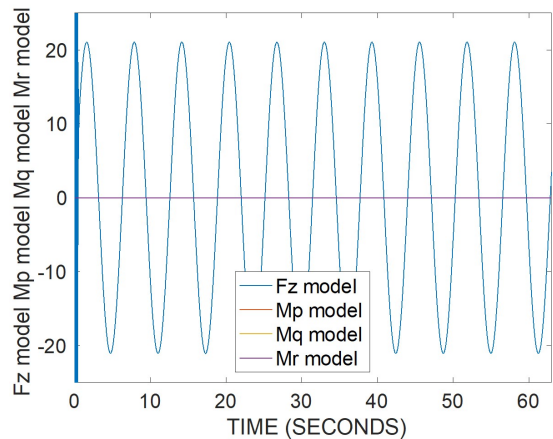


Fig. 6. $F_{zmodel}, M_{pmodel}, M_{qmodel}, M_{rmodel}$ for tracking the trajectory of the multi-rotor UAV.

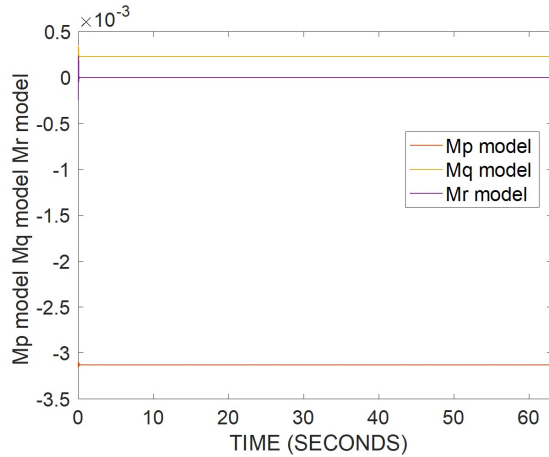


Fig. 7. M_{pmodel} , M_{qmodel} , M_{rmodel} for tracking trajectory of the multi-rotor UAV.

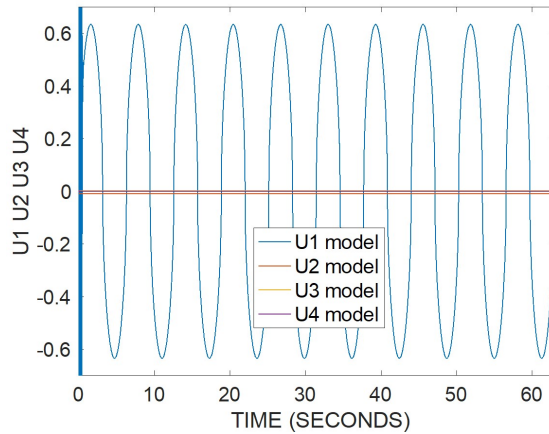


Fig. 8. U_{1model} , U_{2model} , U_{3model} , U_{4model} for tracking the trajectory of the multi-rotor UAV.

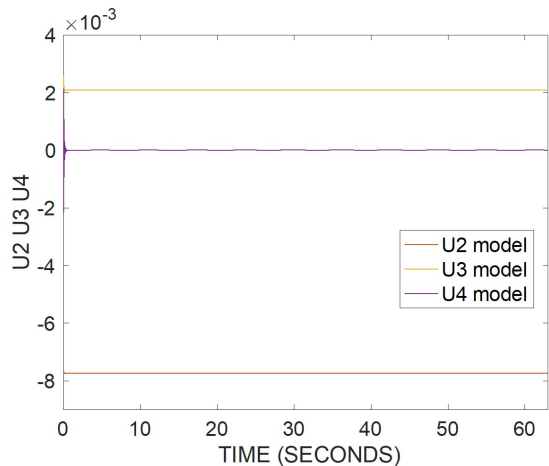


Fig. 9. U_{2model} , U_{3model} , U_{4model} for tracking the trajectory of the multi-rotor UAV.

Performing an approximation $FAN_b(s)$ of a nonlinear somatic operation type sigmoidal \tilde{V}_{FAN_b} allows to tune

the poles of the controller $C_{FANPID}(s)$ through the parameter c , and the gains P , I , D , N successfully applying the FAN-LA. The optimized response of the system, Fig. 1, was obtained using the $C_{FANPID}(s)$, improving the results reported in [11] and those obtained with the FOPID-Lyapunov-Self-tuning controller, Figs. 2-5. Figs. 6-9 prove that in addition to obtaining the optimization of the response of the FACL system, the F_{zmodel} , M_{pmodel} , M_{qmodel} , M_{rmodel} and the U_{1model} , U_{2model} , U_{3model} , U_{4model} can be estimated applying the low-scale multi-rotor UAV model. By tuning the parameters and determining the system variables, the FACL successfully tracked the trajectory for a low-scale multi-rotor UAV.

6. CONCLUSIONS

The FACL for the trajectory tracking system [28] of a low-scale multi-rotor UAV, using a novel FANPID-Lyapunov controller that applies a Laplace domain approach at FAN model and the FAN-LA, obtained very good results. FANPID controller has the advantage that the gains and parameter can be tuned by applying a fuzzy learning algorithm. The requirement to define initial conditions to tune the gains and parameter of the FAN-LA, is a disadvantage. The error was successfully reduced based on the new FANPID-Lyapunov controller with adaptive or self-tuned gains and parameter compared to a traditional PID-Fixed-gains, a PID-Fuzzy adaptive-gains, a PID-Lyapunov-Fixed-gains and a FOPID-Fuzzy adaptive gains and parameters [17,19,20,35]. The implementation of FACL at commercial processor is proposed for future work. Potential research is in nonlinear and control systems for motors, small-scale UAV, manufacturing processes and tank level, among others.

REFERENCES

- [1] L. Amezcua-Brooks, E. Liceaga-Castro, M. Gonzalez-Sanchez, O. Garcia-Salazar, and D. Martinez-Vazquez, "Towards a standard design model for quad-rotors: A review of current models, their accuracy and a novel simplified model," *Progress in Aerospace Sciences*, vol. 95, pp. 1-23, November 2017.
- [2] L. Amezcua-Brooks, D. Hernandez-Alcantara, C. Santana-Delgado, R. Covarrubias-Fabela, O. Garcia-Salazar, and A. M. E. Ramirez-Mendoza, "Improved model for micro-UAV propulsion systems: Characterization and applications," *IEEE Transactions on Aerospace and Electronic Systems*, vol. 56, no. 3, pp. 2174-2197, 2020.
- [3] J. J. Corona-Sánchez and H. Rodríguez-Cortés, "Trajectory tracking control for a rotary wing vehicle powered by four rotors," *Journal of Intelligent & Robotic Systems*, vol. 70, pp. 39-50, 2013.
- [4] O. Mofid, S. Mobayen, and W.-K. Wong, "Adaptive terminal sliding mode control for attitude and position tracking

- control of quadrotor UAVs in the existence of external disturbance,” *IEEE Access*, vol. 9, pp. 3428-3440, 2021.
- [5] N. Wang, S.-F. Su, M. Han, and W.-H. Chen, “Backpropagating constraints-based trajectory tracking control of a quadrotor with constrained actuator dynamics and complex unknowns,” *IEEE Transactions on Systems, Man, and Cybernetics: systems*, vol. 49, no. 7, pp. 1322-1337, 2019.
- [6] N. Wang and C. K. Ahn, “Coordinated trajectory tracking control of a marine aerial-surface heterogeneous system,” *IEEE/ASME Transactions on Mechatronics*, vol. 26, no. 6, pp. 3198-3210, 2021.
- [7] X. Chen, T. Huang, J. Cao, J. H. Park, and J. Qiu, “Finite-time multi-switching sliding mode synchronization for multiple uncertain complex chaotic systems with network transmission mode,” *IET Control Theory & Applications*, vol. 13, no. 9, pp. 1246-1257, 2019.
- [8] K. Elikier and W. Zhang, “Finite-time adaptive integral backstepping fast terminal sliding mode control application on quadrotor UAV,” *International Journal of Control, Automation, and Systems*, vol. 18, no. 2, pp. 415-430, 2020.
- [9] L. Yu, G. He, S. Zhao, X. Wang, and L. Shen, “Immersion and invariance-based sliding mode attitude control of tilt tri-rotor UAV in helicopter mode,” *International Journal of Control, Automation, and Systems*, vol. 19, no. 2, pp. 722-735, 2021.
- [10] T. Huang, D. Huang, Z. Wang, X. Dai, and A. Shah, “Generic adaptive sliding mode control for a quadrotor UAV system subject to severe parametric uncertainties and fully unknown external disturbance,” *International Journal of Control, Automation, and Systems*, vol. 19, no. 2, pp. 698-711, 2021.
- [11] C. Wang, X. Chen, J. Cao, J. Qiu, Y. Liu, and Y. Luo, “Neural network-based distributed adaptive pre-assigned finite-time consensus of multiple TCP/AQM networks,” *IEEE Transactions on Circuits and Systems*, vol. 68, no. 1, pp. 387-395, January 2021.
- [12] Y. Kao, Y. Li, J. H. Park, and X. Chen, “Mittag-Leffler synchronization of delayed fractional memristor neural networks via adaptive control,” *IEEE Transactions on Neural Networks and Learning Systems*, vol. 32, no. 5, pp. 2279-2284, May 2021.
- [13] G. Michieletto, A. Cenedese, L. Zaccarian, and A. Franchi, “Hierarchical nonlinear control for multi-rotor asymptotic stabilization based on zero-moment direction,” *Automatica*, vol. 117, pp. 1-13, 2020.
- [14] J. L. Sanchez-Lopez, M. Castillo-Lopez, M. A. Olivares-Mendez, and H. Voos, “Trajectory tracking for aerial robots: An optimization-based planning and control approach,” *Journal of Intelligent & Robotic Systems*, vol. 100, pp. 531-574, 2020.
- [15] M. Rabah, A. Rohan, S. A. S. Mohamed, and S.-H. Kim, “Autonomous moving target-tracking for a UAV quadcopter based on fuzzy-PI,” *IEEE Access*, vol. 7, pp. 38407-38419, 2019.
- [16] R.-J. Wai and A. S. Prasetya, “Adaptive neural network control and optimal path planning of UAV surveillance system with energy consumption prediction,” *IEEE Access*, vol. 7, pp. 126137-126153, 2019.
- [17] A. M. E. Ramírez-Mendoza, J. R. Covarrubias-Fabela, L. A. Amezcua-Brooks, O. García-Salazar, and W. Yu, “Fuzzy adaptive neurons applied to the identification of parameters and trajectory tracking control of a multi-rotor unmanned aerial vehicle based on experimental aerodynamic data,” *Journal of Intelligent & Robotic Systems*, vol. 100, pp. 647-665, 2020.
- [18] D. Horla, W. Giernacki, T. Báca, V. Spurny, and M. Saska, “AL-TUNE: A family of methods to effectively tune UAV controllers in in-flight conditions,” *Journal of Intelligent & Robotic Systems*, vol. 103, no. 5, pp. 1-16, 2021.
- [19] M. Gheisarnejad and M. H. Khooban, “An intelligent non-integer PID controller-based deep reinforcement learning: Implementation and experimental results,” *IEEE Transactions on Industrial Electronics*, vol. 68, no. 4, pp. 3609-3618, April 2021.
- [20] J. Z. Shi, “A fractional order general type-2 fuzzy PID controller design algorithm,” *IEEE Access*, vol. 8, pp. 52151-52172, 2020.
- [21] L.A. Zadeh, *Theory of Fuzzy Sets, Encyclopedia of Computer Science and Technology*, Marcel Dekker, Nueva York, E.U.A., 1977.
- [22] D. Dubois and H. Prade, “Towards fuzzy differential calculus. Part1: Integration of fuzzy mappings,” *Fuzzy Sets and Systems*, vol. 8, pp. 1-17, 1982.
- [23] W. Yu and X. Li, “Fuzzy identification using fuzzy neural networks with stable learning algorithms,” *IEEE Transactions on Fuzzy Systems*, vol. 12, no. 3, pp. 411-420, 2004.
- [24] A. M. E. Ramírez-Mendoza and W. Yu, “Simplified model of the propulsion system for a PVTOL with a disturbance and estimate of power efficiency,” *DYNA*, vol. 97, no. 5, pp. 470-474, 2022.
- [25] M. M. Gupta and D. H. Rao, “On the principles of fuzzy neural networks,” *Fuzzy Sets and Systems*, vol. 61, pp. 1-18, 1994.
- [26] J. L. Pérez and A. Ramírez, “Two new models of integrative fuzzy neuron,” *Instrumentation & Development*, vol. 5, no. 3, pp. 140-145, 2001.
- [27] A. Ramírez-Mendoza, J. L. Pérez-Silva, and F. Lara-Rosano, “Electronic implementation of a fuzzy neuron model with a Gupta integrator,” *JART-Journal of Applied Research and Technology*, vol. 9, no. 3, pp. 380-393, 2011.
- [28] A. Ramírez-Mendoza, “Study of the response of the connection of adaptive fuzzy spiking neurons with self-synapse in each single neuron,” *Proc. of 11th International Conference on Electrical Engineering, Computing Science and Automatic Control*, pp. 1-6, 2014.
- [29] A. M. E. Ramírez-Mendoza, J. R. Covarrubias-Fabela, L. A. Amezcua Brooks, and D. Hernández-Alcántara, “Parameter identification using fuzzy neurons: Application to drones and induction Motors,” *DYNA*, vol. 93, no. 1, pp. 75-81, 2018.
- [30] A. M. E. Ramírez-Mendoza, “Modeling the spike response for adaptive fuzzy spiking neurons with application to a fuzzy XOR,” *Computer Modeling in Engineering & Sciences*, vol. 115, no. 3, pp. 295-311, 2018.

- [31] A. M. E. Ramírez-Mendoza, W. Yu, and X. Li, "A novel fuzzy system with adaptive neurons for earthquake modeling," *IEEE Access*, vol. 8, no. 1, pp. 101369-101376, 2020.
- [32] A. M. E. Ramírez-Mendoza, W. Yu, and X. Li, "Fuzzy identification of systems based on adaptive neurons," *Journal of Intelligent & Fuzzy Systems*, vol. 40, pp. 10767-10779, 2021.
- [33] A. M. E. Ramírez-Mendoza and W. Yu, "A novel learning algorithm for adaptive fuzzy neural networks: Application to the neuro-fuzzy design of control law for a PID controller," *Soft Computing*, (under review).
- [34] A. M. E. Ramírez-Mendoza, W. Yu, and X. Li, "A new spike membership function for the recognition and processing of spatiotemporal spike patterns: Syllable-based speech recognition application," *Fuzzy Sets and Systems*, (under review).
- [35] H. K. Khalil, *Nonlinear Systems*, Prentice Hall, p. 750, 2002.
- [36] M. V. Cook, *Flight Dynamics Principles*, Elsevier Ltd., Great Britain, pp. 18-21, 2007.



Abigail María Elena Ramírez Mendoza

received her B.S. degree in mechanical electrical engineering from National Autonomous University of Mexico (UNAM for its acronym in Spanish) in 1996, master and Ph.D. degrees in Engineering degrees, from UNAM, Mexico, in 1998 and 2013, respectively. From 2015-2018, she was a distinguished researcher with a CONA-

CYT Research Fellowship - Autonomous University of Nuevo León (UANL for its acronym in Spanish), Mexico. From 2013-2014 and 2019-2020, she obtained a Postdoctoral Stay at the Department of Automatic Control at CINVESTAV-IPN, Mexico. Professor at Department of Electromechanical Engineering, ITSOEH, Mexico, 2021-2022. She is currently doing a Postdoctoral stay at the Department of Autonomous Air and Submarine Navigation Systems, LAFMIA UMI, CINVESTAV-IPN. Her research interests include fuzzy neurons, fuzzy adaptive control, and system identification.



Wen Yu received his B.S. degree in automatic control from Tsinghua University, Beijing, China in 1990 and his M.S. and Ph.D. degrees, both in electrical engineering, from Northeastern University, Shenyang, China, in 1992 and 1995, respectively. Since 1996, he has been at CINVESTAV-IPN, Mexico City, Mexico, where he is currently a Professor at Department of Automatic Control. Dr. Wen Yu serves as Associate Editor of IEEE Transactions on Cybernetics, Neurocomputing, and Journal of Intelligent and Fuzzy Systems. He is a member of the Mexican Academy of Sciences.